Proceedings of the Indian National Science Academy (2023) 89:902–913
https://doi.org/10.1007/s43538-023-00200-x

RESEARCH PAPER

Deciphering the structural insights of the attachment glycoprotein of HeV-g2, a new variant of Henipavirus through homology modeling and molecular dynamics simulation

Norine Dsouza[1,2] · Shivank Sadasivan[2] · Selvaa Kumar Chellasamy[1]

Received: 30 May 2023 / Accepted: 11 August 2023 / Published online: 14 September 2023

Abstract
Henipavirus harbors both pathogenic Hendra and Nipah viruses that infect humans and livestock animals. Recently, a variant of the Henipavirus, HeV-g2, has been discovered in horses and bats. Compared with the other Henipaviruses, the role of HeV-g2 proteins in host interaction is poorly understood to date. The present study focuses on the comparative sequence and structural analysis of the attachment glycoprotein of HeV-g2 with the members of the Henipavirus, which would provide valuable insights to understand its structural dynamics and functions. After retrieving the attachment glycoprotein sequence of HeV-g2, the evolutionary analysis was performed with protein sequences of members of Henipavirus, which showed a higher resemblance with Hendra and Nipah viruses confirming the possible pathogenic nature. Functionally, the EFNB2 host receptor binding site of the HeV-g2 attachment protein showed maximum amino acid residue conservation except for five residues of NiV: *Ser242Thr*, *Gln388Lys*, *Phe458Tyr*, *Ile502Val*, *Asn586Ser,* and single residue *Val401Ile* of HeV. The modeled structure of the protein when subjected to molecular simulation studies showed a similar pattern of structural stability with HeV protein, measured in terms of Root Mean Square Deviation, Root Mean Square Fluctuation (RMSF) Radius of Gyration (RoG), Solvent accessible surface area (SASA) and hydrogen bonding pattern. Our study highlighted the sequence comparability and structural dynamics of modeled attachment glycoprotein of HeV-g2 and the information obtained on the functional and structural regions can be considered for further research in order to design better inhibitors for the infection caused by this virus.

Keywords HeV-g2 · Attachment glycoprotein · EFNB2 binding · Hendra · Nipah

Introduction

The viral infectious disease outbreaks leading to epidemics and pandemics are the major threats to the well-being of humans. The pathogenic viruses infecting different hosts belong to more than 15 families and the single-stranded negative-sense RNA viral family *Paramyxoviridae* contains several species of viruses infecting humans (Carrasco-Hernandez et al. 2017; Siegel 2018). Henipavirus, a genus of the *Paramyxoviridae* family comprises of Nipah virus (*NiV*), Hendra virus (HeV), Cedar virus (CedV), Ghana virus (GhV), *Mòjiāng* virus (MojV), and Langya virus (LayV) (Quarleri et al. 2022; Aguilar and Lee 2011). Among the Henipaviruses, HeV and NiV are the zoonotic agents known to be highly infectious to humans and livestock animals with severe neuropathological symptoms, and a case fatality rate ranging between 40 and 80% (Marsh and Wang 2012; Halpin and Rota 2015). The ability of HeV and NiV to infect domesticated and livestock animals from six different mammalian orders adds to the list of priority viruses. (Kummer and Kranz 2022; Weingartl 2015; Glennon et al. 2018). Owing to its range of hosts, the nature of infections, and the mortality rate, NiV, and HeV presence were monitored through multiple surveillance studies (Plowright et al. 2019; Adamu et al. 2022; Wacharapluesadee et al 2021). A surveillance study conducted between 2013 and 2021 detected a novel member, HeV genotype2 virus (HeV-g2)

✉ Selvaa Kumar Chellasamy
selvaakumar.c@dypatil.edu

1 School of Biotechnology and Bioinformatics, D.Y. Patil Deemed to be University, CBD Belapur, Navi Mumbai, Maharashtra 400614, India

2 Department of Biotechnology, St. Xavier's College, Mumbai, Maharashtra, India

in Grey-headed flying foxes (GHFF) from Australia. Studies conducted to ascertain the viral identity through comparative genome analysis revealed an 83.6% sequence identity with the HeV followed by a 71% identity with NiV isolates suggesting the potential pathogenic nature of the *HeV-g2* (Wang et al. 2021). Likewise, a second variant of HeV was detected in an infected horse from the Newcastle region of Australia (Taylor et al. 2022). Upon comparison with other Henipaviruses, this newly discovered virus showed similarity with HeV suggesting a risk of spillover infection and circulation of HeV variants among the natural hosts (Taylor et al. 2022).

Further, experimental studies conducted using the newly identified *HeV-g2* showed a comparable human receptor binding ability similar to the *HeV* virus, which uses EFNB2 and EFNB3 as the host cell receptor to gain entry into the cell. (Wang et al. 2022; Peel et al. 2022). Evidently, in HeV and NiV the attachment glycoprotein is one of the first proteins which establishes the host-cell interaction (Xu et al. 2012a, b; Laing et al. 2019) and this ability of the attachment glycoprotein has been exploited in vaccine candidates, small molecular therapeutics designing, and development (Loomis et al. 2020; Xu et al. 2012a; Broder et al. 2013; Bradel-Tretheway et al. 2019). Attempts made to develop a vaccine using *HeV* attachment glycoprotein provided immunogenetic protection to HeV and NiV in African green monkeys in experimental studies (Bossart et al. 2012). Moreover, the single-dose HeV and NiV glycoprotein-based subunit vaccine has been developed against Henipaviral infection which is in phase I clinical trial studies (Geisbert et al. 2021). The currently available studies highlight the importance of attachment glycoprotein in mediating viral entry and as a therapeutic target in multiple paramyxoviruses including HeV and NiV (Bose et al. 2015). The Henipavirus genera of paramyxovirus also pose a greater threat to humans and livestock animals in terms of health and economic losses (Kummer and Kranz 2022). The inadequacy of effective vaccines and drugs makes these viruses high-priority viruses for finding suitable treatment regimens and preventive measures (Skowron et al. 2022). The recent detection of new members with high pathogenicity emphasizes the need to prioritize the studies on the HeV-g2 variant. Thus the present study focuses on determining the structural architecture of attachment glycoprotein from newly reported HeV-g2 using the in-silico methods, with the pathogenic members HeV and NiV to decipher the functional role. The study can provide valuable molecular insights into understanding the role of attachment glycoprotein in the HeV-g2 and facilitate the development of suitable attachment glycoprotein inhibitors and vaccine candidates against the newly discovered virus.

Materials and methods

Comparative sequence analysis of attachment glycoprotein

To compare the HeV-g2 attachment glycoprotein with the other members of the genus Henipavirus, we selected 10 sequences of attachment glycoprotein and retrieved the data from NCBI's GenBank database (https://www.ncbi.nlm.nih.gov/genbank/) and UniProtKB database (https://www.uniprot.org/) with the accession numbers UCY33688, UCY33679.1, UCY33670.1, UYS87243.1 (HeV-g2), UUV47241 (LayV), O89343 (HeV), Q9IH62 (NiV), J7H333 (CedV), W8TIR7 (MojV) and, I0E093 (GhV). The selected attachment glycoprotein sequences were aligned using ClustalW multiple sequence alignment program and the aligned sequences were used for phylogenetic tree construction using MEGA 11 software. The neighbor-joining statistical clustering method and the test for phylogeny using the bootstrap method with 1000 replicates were employed (Tamura et al. 2021).

Based on the phylogenetic analysis results, the closely related clade to HeV-g2, consisting of HeV, and NiV were realigned using Clustal omega (Sievers et al. 2011), and the percentage identity score was calculated. To identify the residue conservation in the host receptor binding sites of attachment glycoproteins, the aligned sequences were imported to the Jalview editor (Waterhouse et al. 2009), and the pattern of conservation was recorded.

Comparative analysis of physicochemical properties of attachment glycoprotein HeV-g2

To analyze the physicochemical properties of HeV-g2 attachment glycoprotein, we selected only a single sequence, UCY33688 owing to its identity with the other members of HeV-g2. To compare the physicochemical properties, we also selected O89343 (HeV), and Q9IH62 (NiV) reference sequences and the for analysis, Pepstats (https://www.ebi.ac.uk/Tools/seqstats/emboss_pepstats/), Protparum (https://web.expasy.org/protparam/) web servers were used. Using these two servers a comparative analysis of molecular weight, isoelectric point, Grand Average Hydrophilicity (GRAVY), aliphatic index, instability index, and the composition of polar/nonpolar and charged was analyzed. Furthermore, to obtain information on changes in composition, charge, and hydrophobicity across the length of the protein sequences VOLPES-visualization of physicochemical sequence properties (http://volpes.univie.ac.at/) webserver was employed.

Three-dimensional structure prediction for HeV-g2 attachment glycoprotein and validation

To analyze the structural dynamics of HeV-g2 attachment glycoprotein, a three-dimensional structure prediction was done using the SWISS-MODEL server which uses the homology modeling approach to predict the structure (Waterhouse et al. 2018). The HeV-g2 protein sequence UCY33688 was used as the query sequence and the attachment glycoprotein structure of HeV (PDB ID: 6PDL) with an identity of 92.83% was used as a template. The modeled structure was validated using ProSAweb (https://prosa.services.came.sbg.ac.at/prosa.php) and Procheck (https://saves.mbi.ucla.edu/).

Molecular dynamic (MD) simulation studies on HeV-g2 attachment glycoprotein

To understand the dynamic nature of the protein we subjected the HeV-g2 modelled structure to MD simulation studies. To compare structural properties, the three-dimensional attachment glycoprotein structures of HeV (6PDL) and NiV (2VSM) were used as references. The MD simulations were performed using GROMACS 5.0.2 suite (Abraham et al. 2015). The initial topology files using the pdb-2gmx module and OPLS-AA force field were employed to generate the topologies. The TIP3P water model was chosen to solvate the protein in a 1 nm cubic box and the system was solvated with a total of 35,934 solvent molecules. A total of two sodium counterions were used to neutralize the solvated system. To eliminate the boundary effect periodic boundary condition (PBC) was imposed and the energy minimization procedure using the steepest descent algorithm using 50,000 steps, was employed to eliminate the clashes in the protein and bad contacts. The energy-minimized system was pre-equilibrated using NVT and NPT ensembles at a temperature of 300 K and 1 atm pressure for 500 ps. Following the temperature and pressure equilibration, the production of the MD run was performed with no restraints for 100 ns. The time step was set for 2 fs and the trajectories were saved for every 100 ps (Lemkul 2018). A similar protocol was run on HeV and NiV glycoprotein and all the runs were performed in triplicates.

Comparative analysis of structural deviation of HEV-g2 attachment glycoprotein with the reference protein structures (HeV and NiV) was analyzed using MD trajectories for Root mean square deviation (RMSD) of protein (backbone) root mean square fluctuation (RMSF) of amino acid residues, Radius of gyration (RoG), Solvent accessible surface area (SASA), the total number of hydrogen bonds. The utility packages gmx rms, gmx rmsf, gmx gyrate, gmx sasa, and gmx hbonds in GROMACS were used for analysis and the graphs were plotted using xmgrace (Turner 2005).

Secondary structural analysis

The secondary structural pattern of attachment glycoproteins was obtained by using the do_DSSP plugin installed in GROMACS. The software tool DSSP (Database of Secondary Structure in Proteins) was developed by Kabsch and Sander (Carter et al. 2003), which uses the hydrogen bonding pattern along with the geometrical pattern to assign the secondary structure for the protein under study. A comparative analysis of the DSSP was performed for HEV-g2, HeV, and NiV attachment glycoproteins and results are plotted using xmgrace.

Results and discussion

Comparative sequence analysis of attachment glycoprotein

The 10 attachment glycoprotein sequences from different members of Genus Henipavirus were aligned using the Clustal W program in MEGA-11 software. The phylogenetic tree constructed with the neighbor-joining method for the attachment sequences is shown in Fig. 1. The attachment glycoprotein of HeV-g2 isolates showed a close resemblance to HeV, followed by NiV. All the protein sequences of HeV-g2 isolates were very identical and formed a close cluster. The formation of a clade with NiV being the outgroup shows the evolution of HeV-g2 from the pathogenic members.

Extending our study, we also observed a newly discovered Henipavirus LayV, which causes febrile illness in humans, showing a close resemblance with MojV with respect to the attachment glycoprotein, which is in agreement with the genomic comparison studies conducted earlier by Chakraborty et al. 2022. Additionally, the phylogenetic tree also showed a second closely related clade between Mojiang and LayV attachment glycoprotein, a newly discovered Henipavirus causing febrile illness in humans (Chakraborty et al. 2022).

Based on the phylogenetic analysis results, we selected HeV-g2 (UYS87243.1-horse and UCY33688.1-bat), HeV, and NiV attachment glycoprotein sequences and the percentage identity between the sequences is represented in Fig. 2. The attachment glycoprotein of HeV-g2 isolates showed an identity of 99.39%, whereas with HeV and NiV glycoprotein the identity was found to be 92.7%, and 79.53% respectively. The study shows a very close resemblance of HeV-g2 with HeV.

The difference of 7.3% and 20.47% in attachment glycoprotein with HeV and NiV led to the analysis of residue conservation in the host receptor binding sites in attachment glycoprotein sequences. Studies have shown high conservation of amino acid residues among HeV and NiV,

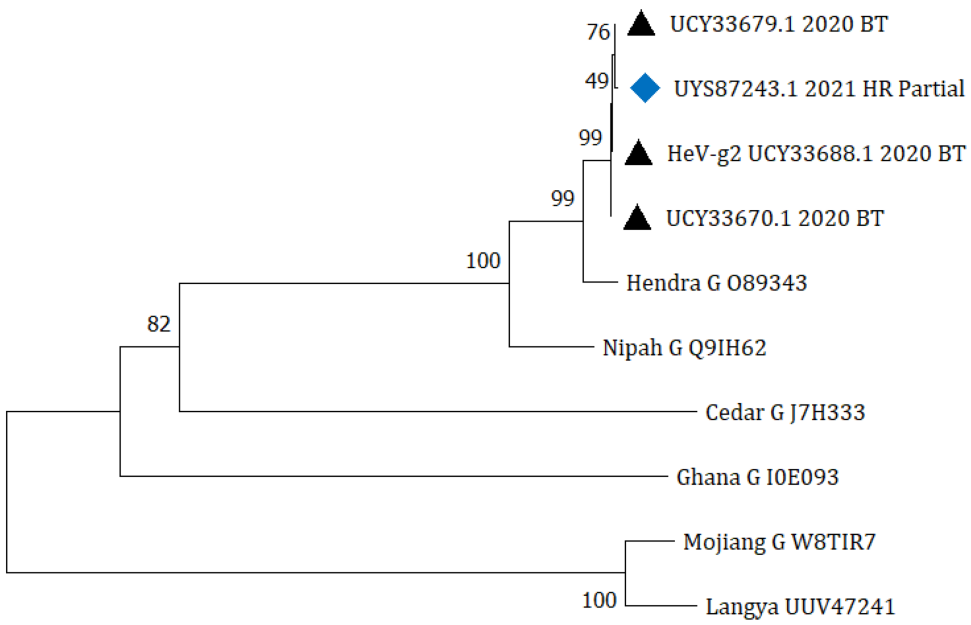

Fig. 1 Evolutionary divergence of Henipaviral attachment glycoprotein. ▲ ◆ Represents the attachment glycoprotein sequences from HeV-g2. *HR* horse and *BT* bat

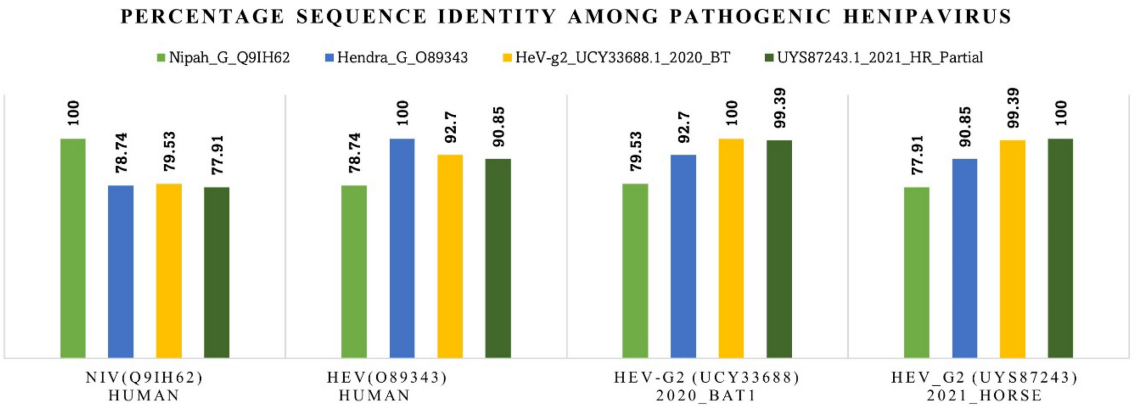

Fig. 2 Comparative percentage sequence identity of attachment glycoprotein of HeV-g2, HeV, and NiV

wherein *Ser239*, *Cys240*, *Ser/Thr241*, *Arg242*, *Leu305*, *Lys/Gln388*, *Tyr389*, *Val/Ile401*, *Tyr/Phe458*, *Pro488*, *Gln490*, *Ser491*, *Gln492*, *Glu501*, *Trp504*, *Glu505*, *Gly506*, *Glu530*, *Thr531*, *Ala532*, *Glu533*, *Asp555*, *Asn557*, *Gln559*, *Ile580*, *Tyr581*, *Asp582*, *Thr583*, and *Ile588* were involved in EFNB2 interaction (Bowden et al. 2008; Xu et al. 2012a, b). Interestingly, the HeV-g2 attachment glycoprotein showed sequence variation with HeV and NiV proteins but the EFNB2 binding site showed high amino acid residue conservation except for five residues of NiV (*Ser242Thr*, *Gln388Lys*, *Phe458Tyr*, *Ile502Val*, *Asn586Ser*) and single residue *Val401Ile* of HeV. In Fig. 3 the EFNB2 binding sites are highlighted in red boxes, and the differences observed in the binding pocket with NiV are marked in blue arrows and HeV in red arrows.

Further, we compared the peripheral amino acid residues in the non-interface region (Wang et al. 2020) in the 5 Å vicinities of EFNB2 receptor binding sites. The variation pattern observed between HeV-g2 and HeV is marked in yellow boxes (Fig. 3) and four regions *Val520Ile*, *Pro550Gln*, *Asp554Glu*, and *Lys560Arg* showed variation. Similarly, *Val245Ile*, *Arg-402Asd*, *Thr498Val*, *Ile517Leu*, *Phe525Tyr*, *Asp527Asn*, *Thr538Ala*, *Arg548Gln*, *Ala549Val*, *Asd564Asp,* and *Lys-571Val* showed variations with NiV and HeV-g2 (Fig. 3 blue boxed region). The non-interface residue conservation was not observed between HeV-g2 and other proteins at positions 386, 553, 560, and 569 (Fig. 3 pink boxed region). The impact of the amino acid residue variability in the 5 Å of attachment glycoprotein receptor binding region needs to be studied experimentally.

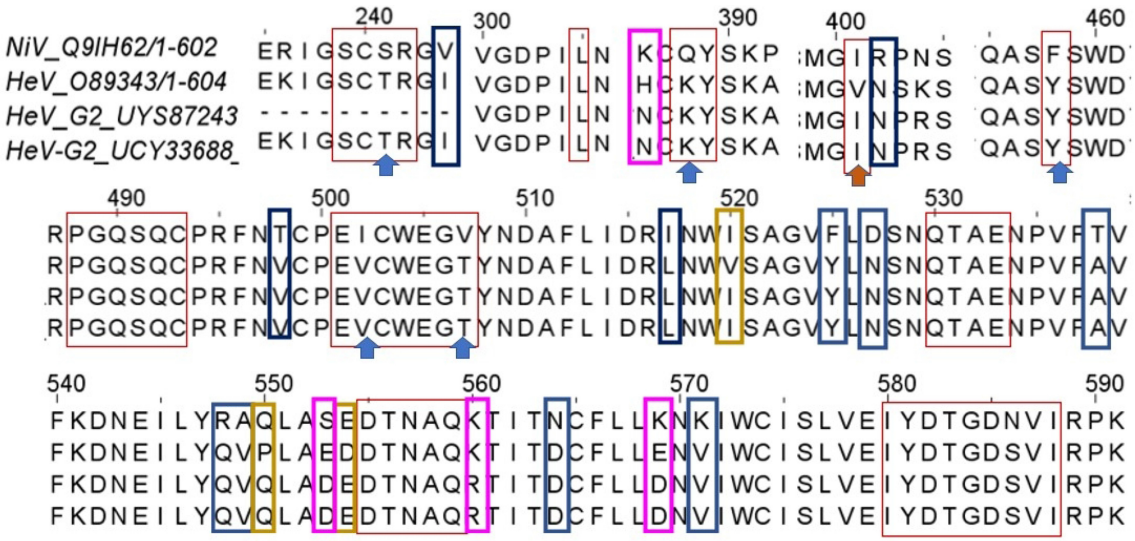

Fig. 3 Regions of amino acids involved in EFNB2 receptor interaction. The red boxes correspond to the EFNB2 binding site. The red and blue arrow corresponds to the variations observed in HeV and NiV

Comparative analysis of physicochemical properties of attachment glycoprotein HeV-g2

The HeV-g2 showed amino acid residue variations with HeV and NiV attachment glycoproteins, and to evaluate the impact of this on various physicochemical properties, we used Protparum and Pepstats web servers. Our comparative analysis of attachment glycoproteins of HeV-g2, HeV, and NiV sequences showed similar molecular weight, percentage polar, non-polar, acidic charged, and basic charged residues. However, the isoelectric point (pI) was found to be different with HeV-g2, showing 8.17 in comparison with HeV (7.42). The Grand Average Hydropathy (GRAVY), where a positive value corresponding to hydrophobic and negative to the hydrophilic nature of the protein (Chang and Yang 2013) was found to be negative for all three proteins indicating the hydrophilic nature of the attachment glycoprotein. Meanwhile, all the proteins with an instability index of less than 40 were found to be stable determined by the composition of dipeptides in a group of proteins (Guruprasad et al. 1990) and it was observed that with the lowest instability index of 32.05, the *HeV-g2* was found to be highly stable for in vitro experimentation. The physicochemical properties of attachment glycoprotein (G) of HeV-g2, HeV, and NiV are shown in Table 1.

Post comparative analysis of physicochemical properties, we focussed on the identification of hotspot regions on the attachment glycoproteins of all three viruses, which showed variations in composition, charge, and hydrophobicity. The regions showing variations in properties are shown in Fig. 4a–c. The major variation in composition is observed between 190–230, 300–340, and 380–425 regions among the protein sequences.

The region between 195–210 and 371–392 in NiV attachment glycoprotein was associated with rabbit anti-NiV-G monoclonal antibody 45 (Mab45) and 26 (Mab26) binding (Stone et al. 2016) and amino acid composition was found to be non-conserved at these regions between HeV-g2 and NiV. The higher amino acid identity between HeV-g2 and HeV also supports its ability to be neutralized by HeV-neutralizing antibodies like hAH1.3, m102.4, and HENV-32 (Wang et al. 2022). Intercomparison of attachment glycoproteins showed changes in the charged amino residues at the 500–580 region between HeV-g2 and NiV;

Table 1 Comparative physicochemical properties of attachment glycoprotein HeV-g2, HeV, and NiV

Viral type	MW	pI	GRAVY	Instability index	Aliphatic index	Polarity		Charge	
						Polar	Nonpolar residues	Acidic	Basic
HeV-g2	67,216.14	8.17	− 0.163	32.05	93.23	281 (46.6%)	322 (53.4%)	56 (9.29%)	67 (11.11%)
HeV	67,191.11	7.42	− 0.130	32.64	95.83	281 (46.52%)	323 (53.48%)	57 (9.44%)	66 (10.93%)
NiV	67,039.03	8.58	− 0.178	34.56	90.95	277 (46.01%)	325 (53.99%)	53 (8.804%)	66 (10.96%)

MW molecular weight, *pI* isoelectric point

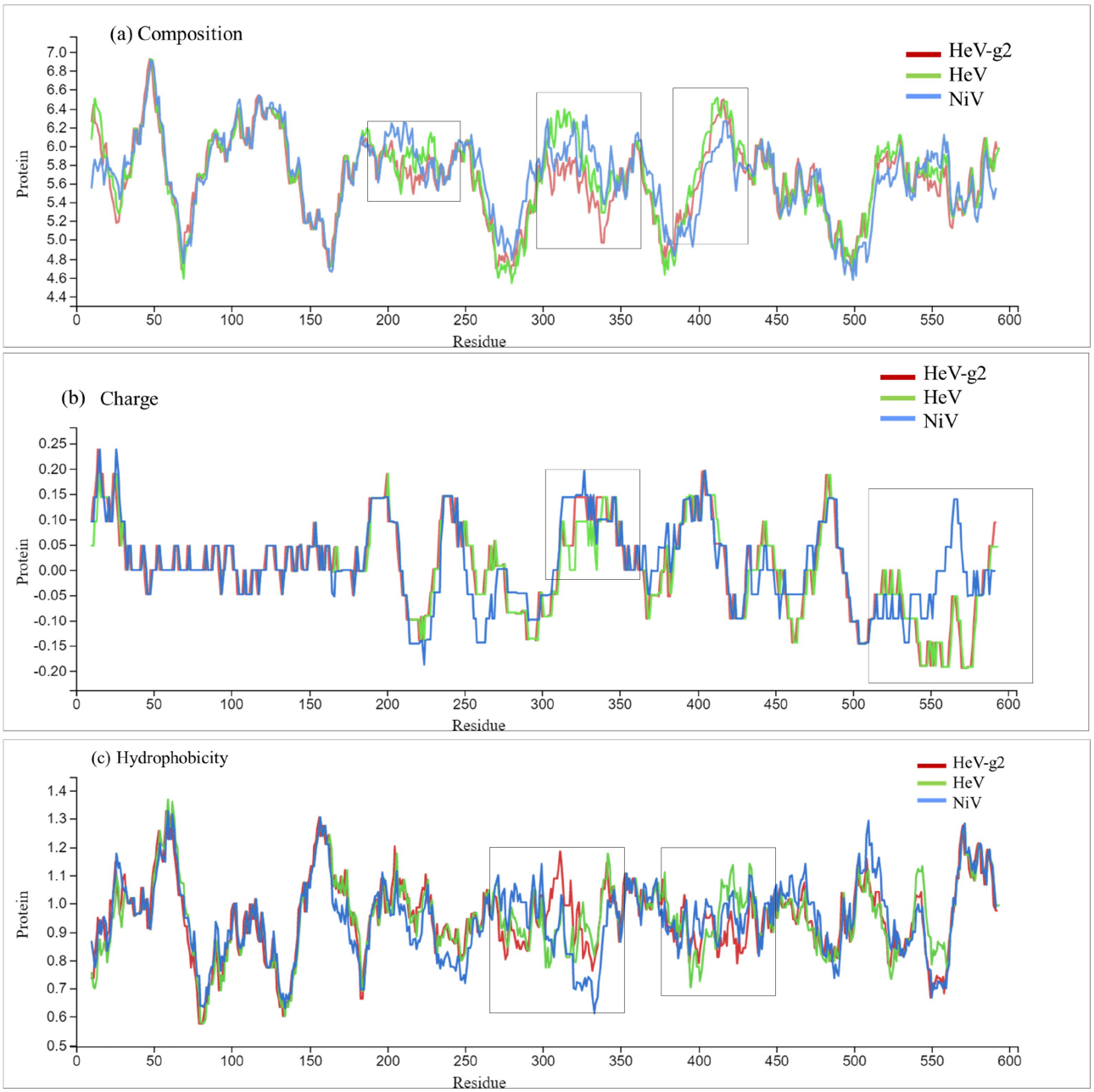

Fig. 4 Comparative amino acid residue properties of HeV-g2, HeV, and NiV. **a** Composition, **b** charge and **c** hydrophobicity variation pattern

the majority of the EFNB2 receptor binding residues (Xu et al. 2012a, b) are mapped to this region of the protein as shown in Fig. 4b.

Meanwhile, a comparative analysis of the hydrophobic properties of attachment glycoproteins revealed the differential pattern of hydrophobic amino acid compositions between 220–350 and 370–450 regions of attachment glycoproteins Fig. 4c.

Three-dimensional structure prediction for HeV-g2 attachment glycoprotein and validation

The three-dimensional structure of attachment glycoprotein for HeV-g2 was predicted using PDB template 6PDL of Hendra virus. The validation of the predicted structure in the ProSA web shows a quality Z-Score of − 7.79, comparable with the protein structures in the PDB database and the

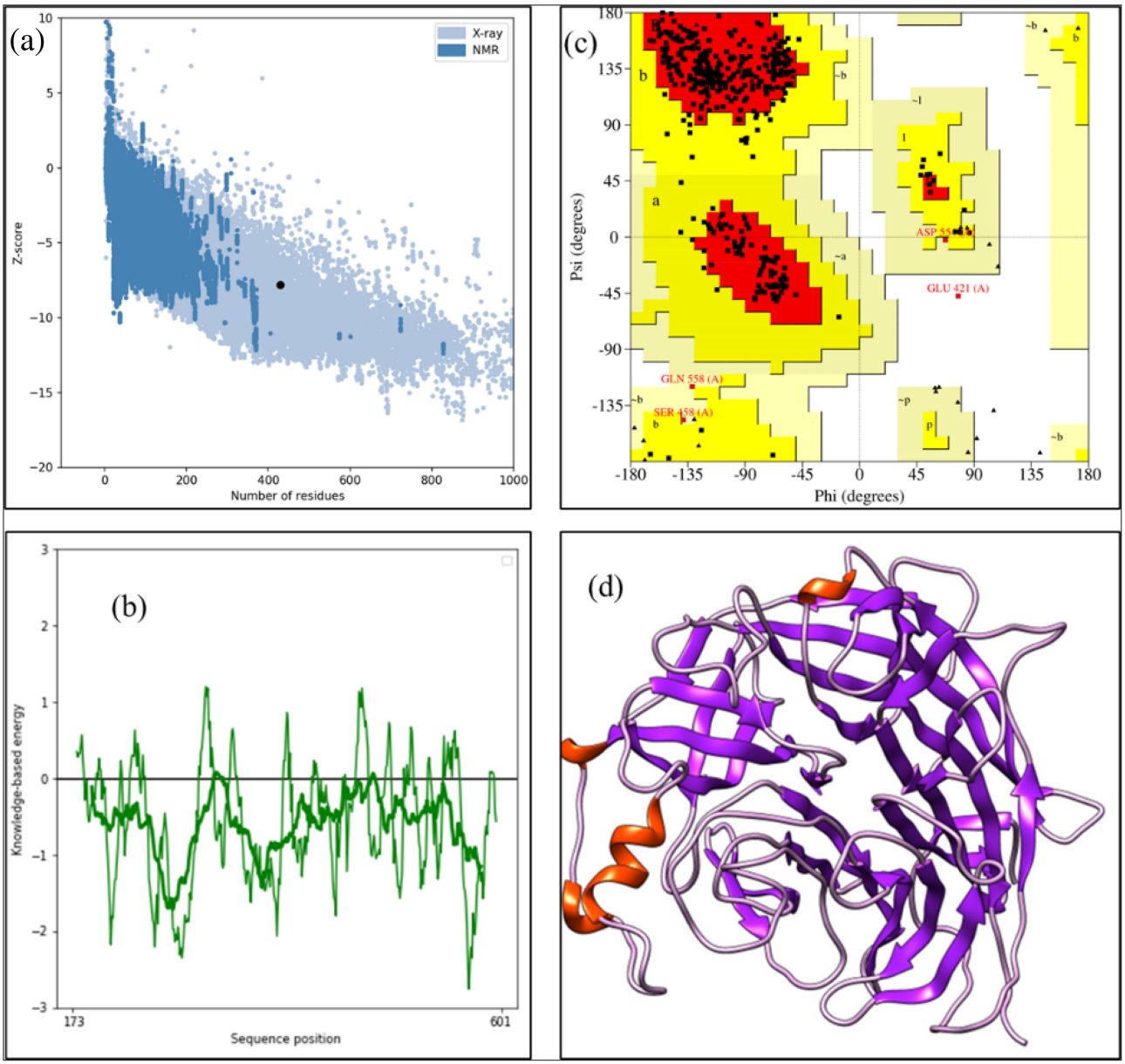

Fig. 5 Three-dimensional structure designing and validation of HEV-g2 protein. **a** Shows the model quality assessed by the ProSA web, **b** the total potential energy of the predicted structure and **c** the Ramachandran plot of the predicted protein; - dark green representing window size 10 and light green representing window size 40. **d** Three-dimensional structure of HeV-g2 with the beta-propeller regions colored in purple

lowest energy plot indicating minimum errors. The overall model quality and the energy plot are shown in Fig. 5a and b. The Ramachandran plot analysis of the predicted structure showed 86.9% of the residues in the allowed region, 12.1% in the additionally allowed region, 0.8% in the generously allowed region, and 0.3% in the disallowed region indicating its suitability for further study. The Ramachandran plot obtained for the predicted structure is shown in Fig. 5c.

The three-dimensional structure predicted for HeV-g2 using the SWISS model is shown in Fig. 5d, which shows the presence of six-bladed β-propeller regions as observed in HeV and NiV attachment glycoproteins (Maar et al. 2012; Bowden et al. 2010).

Molecular dynamic (MD) simulation studies on HeV-g2 attachment glycoprotein

The stability of the predicted HeV-g2 attachment glycoprotein was studied using MD simulations over 100 ns. To get better insights into the protein structure of a newly

discovered virus, a comparative analysis was performed with the well-studied HeV and NiV attachment glycoproteins.

The Root Means Square Deviation (*RMSD*) measures the structural conformation of a protein by calculating the difference between the initial structure and final structure backbone over a period of time (Kufareva and Abagyan 2012). The stability of the protein in the system was evaluated through the calculation of RMSD are represented in Fig. 6a. The HeV-g2 protein reached equilibration with the RMSD of 0.1 nm to 0.15 nm and remained constant throughout the period of simulation. The time taken for all the proteins to reach equilibration was found to be the same, which could be due to the sequence-level similarities between the HeV-g2 with other reference proteins. The HeV-g2 showed an RMSD of 0.16 nm in comparison with 0.15 nm and 0.17 nm of HeV and NiV respectively.

The Radius of Gyration (*RoG*) is a measure of the distribution of protein atoms around the axis indicating the compactness of the protein structure which in turn helps in predicting the structural activity (Sneha and Doss 2016). The comparative RoG values of HeV-g2 with HeV and NiV attachment glycoproteins are shown in Fig. 6b. The Hev-g2 attachment glycoprotein showed an average RoG value of 2.12 nm which was similar to HeV (2.12 nm) and NiV (2.11 nm). The RoG values stabilized between 2.11 and 2.13 nm, which showed the compactness of the protein and proper folding.

Solvent accessible surface area (*SASA*) measures the surface area of the protein accessible to a solvent that provides insights into the distribution of hydrophobic and hydrophilic residues, a key factor in protein folding and stability (Konstantinidis et al. 2021). The modeled HeV-g2 attachment glycoprotein was observed to have 189 nm^2 SASA in comparison with 180 nm^2 and 184 nm^2 of HeV and NiV glycoproteins. The SASA pattern obtained for all the attachment glycoproteins is shown in Fig. 6c. The higher SASA value of HeV-g2 thus is an indicator of the stability of the HeV-g2 proteins.

The protein's secondary and tertiary structural stability is determined by the *hydrogen bonding* pattern, which is the directional interaction and plays an important role in the stabilization of the protein's native structure (Gao et al. 2015).

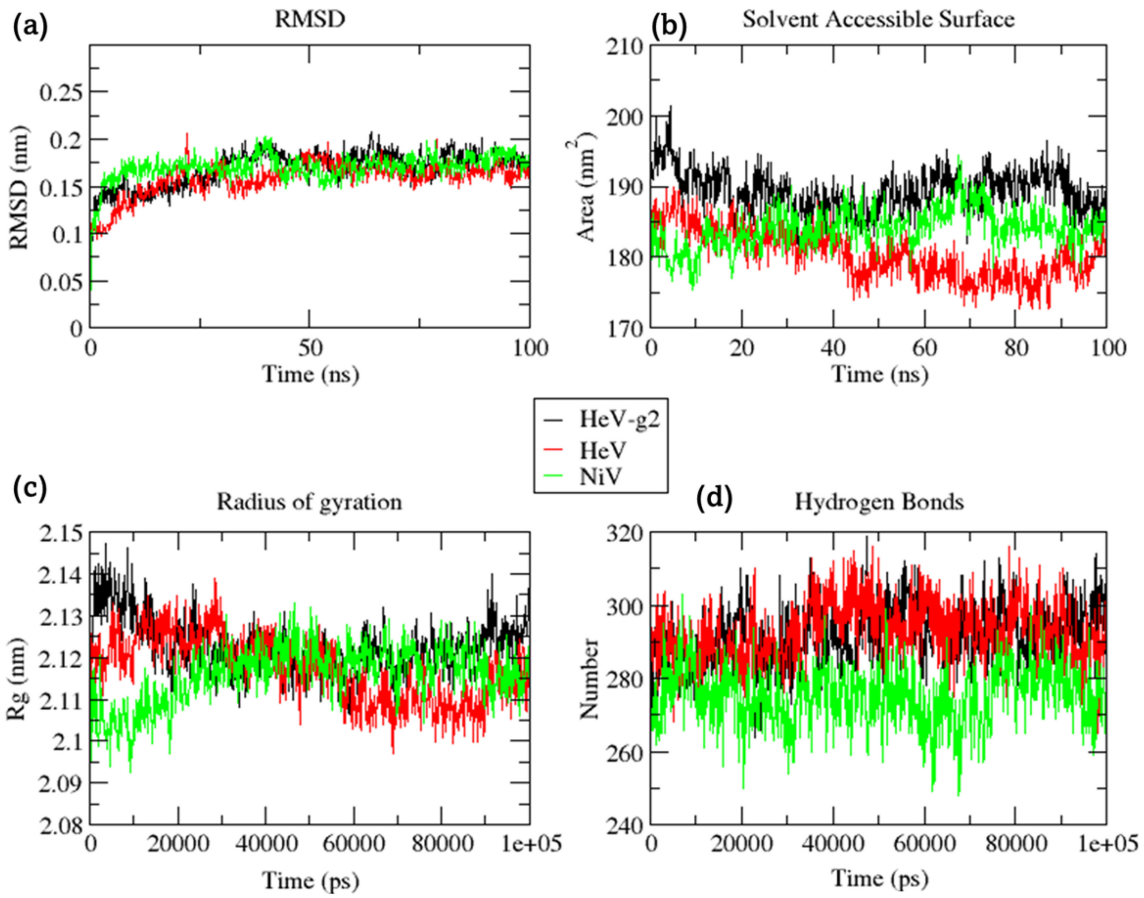

Fig. 6 MD simulation results of attachment glycoprotein of HeV-g2, Hev, and NiV over a time period of 100 ns **a** changes in RMSD, **b** solvent accessible surface area (SASA), **c** radius of gyration, **d** hydrogen bonding. X-axis time in nanoseconds for **a** RMSD and **b** SASA and picoseconds for **c** RoG and **d** hydrogen bonds

Subsequent intramolecular hydrogen bond analysis of HeV-g2 attachment glycoprotein showed an average number of 291 hydrogen bonds which was almost identical to the HeV protein (292). Meanwhile, the NiV attachment glycoprotein showed lesser stability with an average number of 274 hydrogen bonds. The comparative hydrogen bonding pattern for HeV-g2 and reference proteins is shown in Fig. 6d.

Root Means Square Fluctuation (*RMSF*) calculation from MD trajectory assesses the flexibility of individual residues and their movement or fluctuations during the simulation period, with a specific focus on identifying the amino acids in the protein sequence that significantly contribute to structural motion (Abdalla et al. 2022). In the current study, a comparative analysis of the RMSF pattern of attachment glycoprotein of HeV-g2, HeV, and NiV is shown in Fig. 7a. Although several regions in the HeV-g2 attachment glycoprotein showed similar RMSF patterns with the NiV and HeV proteins, the regions exhibiting the fluctuations are highlighted in Fig. 7b–e. To start with, the neutralizing antibody-binding mab45 binds to the region 195–211 in NiV (Aguilar et al. 2009), and this region showed changes in the RMSF values, indicating potential conformational fluctuations and dynamic alterations upon antibody binding. Similarly, most of the amino acid residues binding to the cellular receptor EFNB2 and the cross-reactive neutralizing mAb HENV-26 are found in the range of 480 to 590 of the attachment glycoproteins in HeV and NiV (Dong et al. 2020). The HeV-g2 attachment glycoprotein showed fluctuations at binding regions of EFNB2 and HENV-26 in comparison with the NiV and HeV as shown in Fig. 7c. Overall findings suggest that the observed conformational fluctuations may influence the interactions between these regions and HeV-g2 protein. The comparative physicochemical studies on attachment glycoprotein for hydrophobicity are analyzed previously in Fig. 4c and the RMSF studies also showed fluctuations in this region as shown in Fig. 7d and e. The RMSF studies provide valuable insights into the changes associated with the functional region of the HeV-g2 attachment glycoprotein in comparison with the HeV and NiV proteins. Further experimental studies and functional assays are necessary to fully elucidate the mechanistic details of these interactions and their significance in viral entry and immune evasion strategies.

Dictionary of Secondary Structure of Proteins (*DSSP*)*:* The secondary structure elements are identified for MD-simulated HeV-g2 attachment glycoprotein using the do_DSSP plugin in GROMACS. The analysis provided a comparative DSSP content of attachment glycoprotein from MD trajectory as a function of time. The distribution of secondary

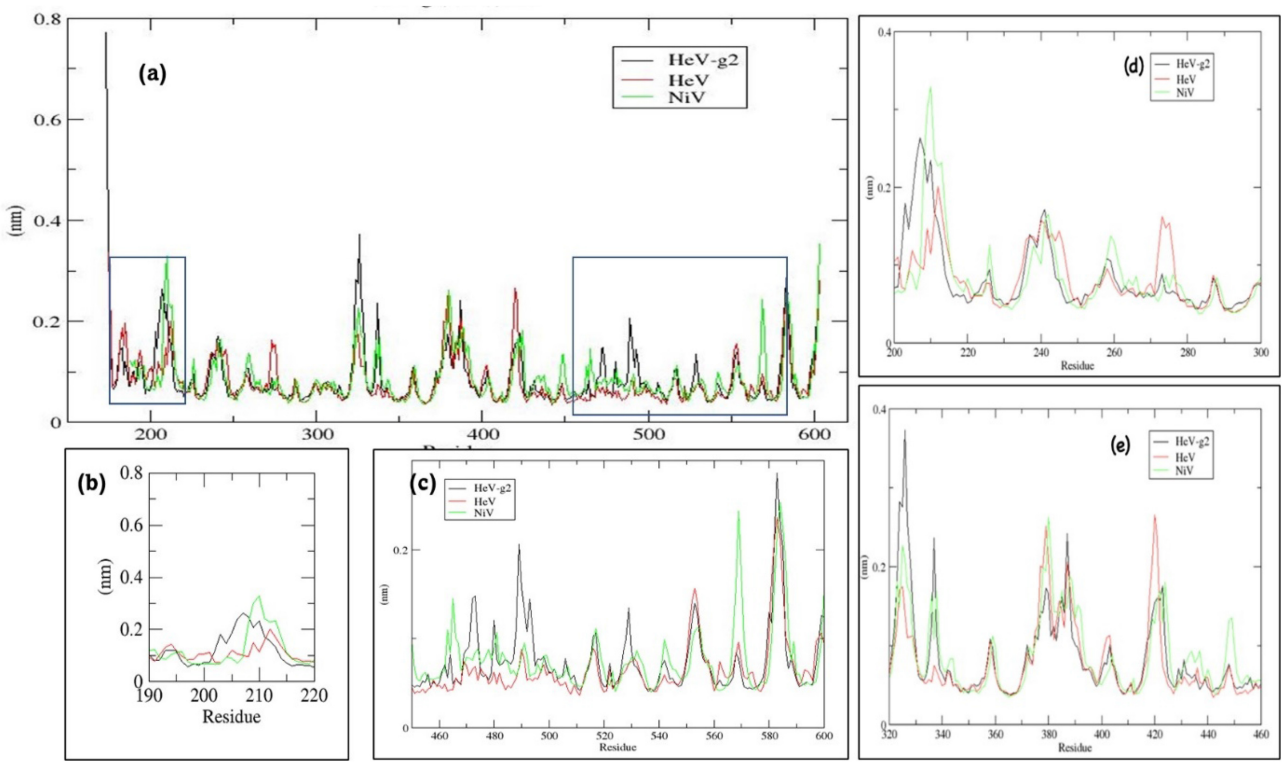

Fig. 7 Comparative RMSF of attachment glycoprotein. **a** comparative RMSF pattern of HeV-g2, HeV, and NiV attachment glycoprotein, **b** residues fluctuation in the antibody integration sites (190–210), **c** residue fluctuation in the EFNB2 binding region, **d** differential pattern of hydrophobic amino acid compositions between 220–350 and **e** 370–450 regions of attachment glycoproteins

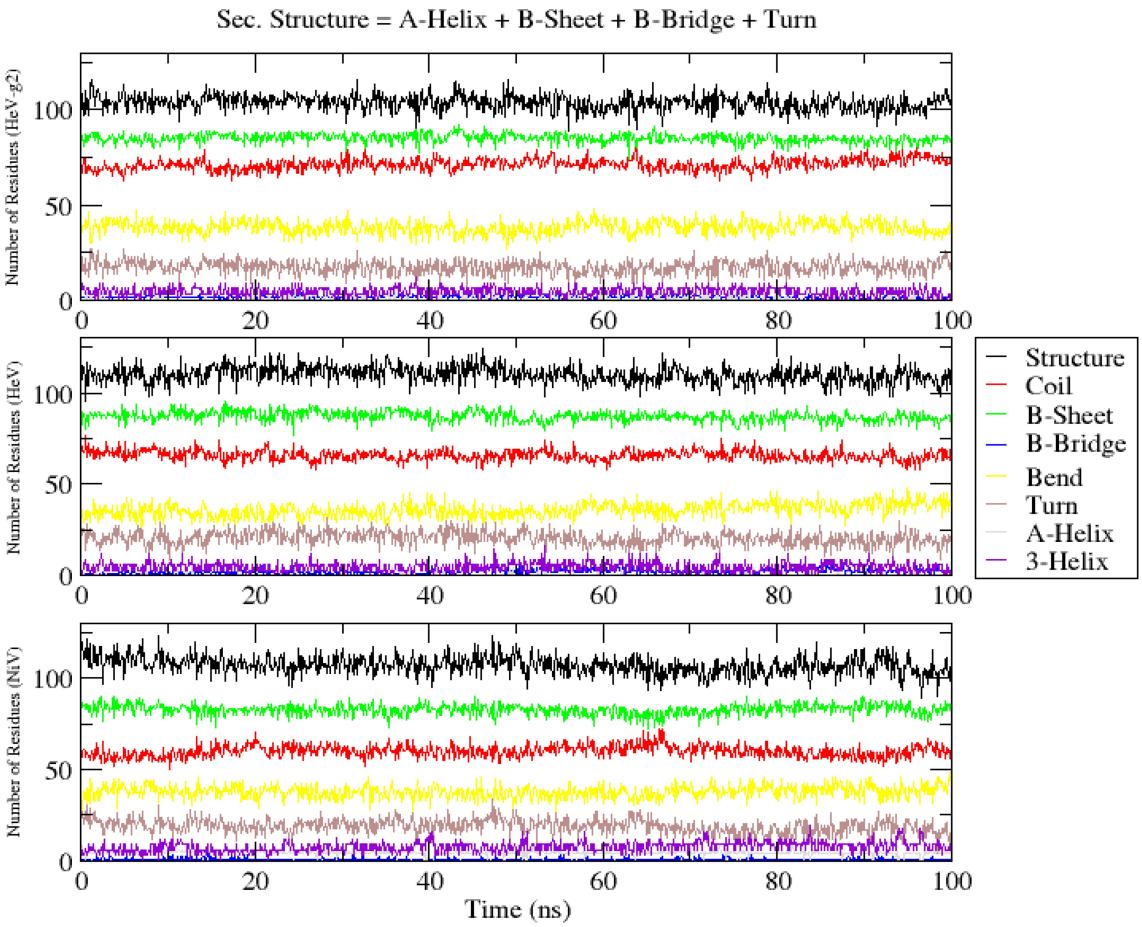

Fig. 8 DSSP analysis for the secondary structure fluctuations as a function of time from 0 to 100 ns for HeV-g2, HeV, and NiV glycoprotein

structural elements for attachment glycoprotein of HeV-g2, HeV, and NiV are shown in Fig. 8.

The HeV-g2 showed predominantly the beta-sheet (green) followed by the coil (red) and high-level secondary structural similarity with HEV attachment glycoprotein was observed. The studies on HeV attachment glycoprotein primarily contain beta sheets which are arranged in the form of 6-blade beta-propeller architecture (Xu et al. 2012a, b). Similarly, the comparison of HeV-g2 with NIV protein showed an identical pattern of beta-sheet distribution except for coils and bends.

In summary, the structural stability and dynamic analysis showed an overall high level of structural conservation of HeV-g2 attachment glycoprotein with HeV followed by NiV.

Conclusion

Comparative studies of the HeV-g2 attachment protein model with HeV and NiV attachment glycoprotein were performed through various in-silico methods. The sequence analysis showed the similarity between HeV-g2, HeV, and NiV, and the differences within binding sites for EFNB2. Structural analysis through MD simulation determined the structural similarities and differences between the three attachment glycoproteins. Overall observations were that the HeV-g2 attachment glycoprotein model has similar properties to HeV and NiV for different structural/functional aspects. This signifies the importance of carrying out a detailed study on HeV-g2 along with HeV and NiV, especially since HeV and NiV have been major epidemiological diseases, threatening the lives of animals and humans in various regions.

Acknowledgements The authors would like to acknowledge the support provided by the School of Biotechnology and Bioinformatics D.Y. Patil Deemed to be University, CBD Belapur, Navi Mumbai, and St. Xavier's College (Autonomous)- DBT-Interdisciplinary Life Science Programme for Advanced Research and Education Builder Grant for providing the computational facility for MD simulations.

Data availability In this study, the protein sequence was derived from the UniProt and NCBI GenBank databases. Their accession numbers are given in the materials and methods section. Similarly, the protein

3D structure was obtained from the Protein Databank with the accession codes provided.

Declarations

Conflict of interest On behalf of all authors, the corresponding author states that there is no conflict of interest.

References

Abdalla, M., Eltayb, W.A., El-Arabey, A.A., Singh, K., Jiang, X.: Molecular dynamic study of SARS-CoV-2 with various S protein mutations and their effect on thermodynamic properties. Comput. Biol. Med. **141**, 105025 (2022). https://doi.org/10.1016/j.compbiomed.2021.105025

Abraham, M.J., Murtola, T., Schulz, R., Páll, S., Smith, J.C., Hess, B., Lindahl, E.: GROMACS: high performance molecular simulations through multi-level parallelism from laptops to supercomputers. SoftwareX **1**, 19–25 (2015). https://doi.org/10.1016/j.softx.2015.06.001

Adamu, A.M., McNabb, L., Adikwu, A.A., Jibril, Y.J., Idoko, S.I., Turaki, A.U., Abalaka, S.E., et al.: Case report: Henipavirus sero-surveillance in horses and pigs from Northern Nigeria. Front. Virol. (2022). https://doi.org/10.3389/fviro.2022.929715

Aguilar, H.C., Lee, B.: Emerging paramyxoviruses: molecular mechanisms and antiviral strategies. Expert Rev. Mol. Med. **13**, e6 (2011). https://doi.org/10.1017/S1462399410001754

Aguilar, H.C., Ataman, Z.A., Aspericueta, V., Fang, A.Q., Stroud, M., Negrete, O.A., Kammerer, R.A., Lee, B.: A novel receptor-induced activation site in the Nipah virus attachment glycoprotein (G) involved in triggering the fusion glycoprotein (F). J. Biol. Chem. **284**(3), 1628–1635 (2009). https://doi.org/10.1074/jbc.M807469200

Bose, S., Jardetzky, T.S., Lamb, R.A.: Timing is everything: fine-tuned molecular machines orchestrate paramyxovirus entry. Virology **479**, 518–531 (2015). https://doi.org/10.1016/j.virol.2015.02.037

Bossart, K.N., Rockx, B., Feldmann, F., Brining, D., Scott, D., LaCasse, R., Geisbert, J.B., et al.: A hendra virus G glycoprotein subunit vaccine protects African green monkeys from Nipah virus challenge. Sci. Transl. Med. **4**(146), 146ra107-146ra107 (2012). https://doi.org/10.1126/scitranslmed.3004241

Bowden, T.A., Aricescu, A.R., Gilbert, R.J., Grimes, J.M., Jones, E.Y., Stuart, D.I.: Structural basis of Nipah and Hendra virus attachment to their cell-surface receptor ephrin-B2. Nat. Struct. Mol. Biol. **15**(6), 567–572 (2008). https://doi.org/10.1038/nsmb.1435

Bowden, T.A., Crispin, M., Harvey, D.J., Jones, E.Y., Stuart, D.I.: Dimeric architecture of the Hendra virus attachment glycoprotein: evidence for a conserved mode of assembly. J. Virol. **84**(12), 6208–6217 (2010). https://doi.org/10.1128/JVI.00317-10

Bradel-Tretheway, B.G., Zamora, J.L., Stone, J.A., Liu, Q., Li, J., Aguilar, H.C.: Nipah and Hendra virus glycoproteins induce comparable homologous but distinct heterologous fusion phenotypes. J. Virol. **93**(13), e00577-e619 (2019). https://doi.org/10.1128/JVI.00577-19

Broder, C.C., Xu, K., Nikolov, D.B., Zhu, Z., Dimitrov, D.S., Middleton, D., Pallister, J., Geisbert, T.W., Bossart, K.N., Wang, L.F.: A treatment for and vaccine against the deadly Hendra and Nipah viruses. Antivir. Res. **100**(1), 8–13 (2013). https://doi.org/10.1016/j.antiviral.2013.06.012

Carrasco-Hernandez, R., Jácome, R., López Vidal, Y., Ponce de León, S.: Are RNA viruses candidate agents for the next global pandemic? A Review. ILAR J. **58**(3), 343–358 (2017). https://doi.org/10.1093/ilar/ilx026

Carter, P., Andersen, C.A., Rost, B.: DSSPcont: continuous secondary structure assignments for proteins. Nucleic Acids Res. **31**(13), 3293–3295 (2003). https://doi.org/10.1093/nar/gkg626

Chakraborty, S., Chandran, D., Mohapatra, R.K., et al.: Langya virus, a newly identified Henipavirus in China-Zoonotic pathogen causing febrile illness in humans, and its health concerns: current knowledge and counteracting strategies–correspondence. Int. J. Surg. (london, England) (2022). https://doi.org/10.1016/j.ijsu.2022.106882

Chang, K.Y., Yang, J.R.: Analysis and prediction of highly effective antiviral peptides based on random forests. PLoS ONE **8**(8), e70166 (2013). https://doi.org/10.1371/journal.pone.0070166

Dong, J., Cross, R.W., Doyle, M.P., Kose, N., Mousa, J.J., Annand, E.J., Borisevich, V., et al.: Potent henipavirus neutralization by antibodies recognizing diverse sites on Hendra and Nipah virus receptor binding protein. Cell **183**(6), 1536–1550 (2020). https://doi.org/10.1016/j.cell.2020.11.023

Gao, Y., Mei, Y., Zhang, J.Z.: Treatment of hydrogen bonds in protein simulations. Adv. Mater. Renew. Hydrog. Prod. Storage Util. **32**, 1854–1858 (2015)

Geisbert, T.W., Bobb, K., Borisevich, V., Geisbert, J.B., Agans, K.N., Cross, R.W., Prasad, A.N., et al.: A single dose investigational subunit vaccine for human use against Nipah virus and Hendra virus. NPJ Vaccines **6**(1), 23 (2021)

Glennon, E.E., Restif, O., Sbarbaro, S.R., Garnier, R., Cunningham, A.A., Suu-Ire, R.D., Osei-Amponsah, R., Wood, J.L., Peel, A.J.: Domesticated animals as hosts of henipaviruses and filoviruses: a systematic review. Vet. J. **233**, 25–34 (2018). https://doi.org/10.1016/j.tvjl.2017.12.024

Guruprasad, K., Reddy, B.B., Pandit, M.W.: Correlation between stability of a protein and its dipeptide composition: a novel approach for predicting in vivo stability of a protein from its primary sequence. Protein Eng. Des. Sel. **4**(2), 155–161 (1990). https://doi.org/10.1093/protein/4.2.155

Halpin, K., Rota, P.A.: A review of Hendra virus and Nipah virus infections in man and other animals. In: Sing, A. (ed.) Zoonoses—infections affecting humans and animals, pp. 997–1012. Springer, Dordrecht (2015). https://doi.org/10.1007/978-94-017-9457-2_40

Konstantinidis, K., Karakasiliotis, I., Anagnostopoulos, K., Boulougouris, G.C.: On the estimation of the molecular inaccessible volume and the molecular accessible surface of a ligand in protein–ligand systems. Mol. Syst. Des. Eng. **6**(11), 946–963 (2021). https://doi.org/10.1039/D1ME00053E

Kufareva, I., Abagyan, R.: Methods of protein structure comparison. Homol. Model. Methods Protoc. (2012). https://doi.org/10.1007/978-1-61779-588-6_10

Kummer, S., Kranz, D.C.: Henipaviruses—a constant threat to livestock and humans. PLoS Negl. Trop. Dis. **16**(2), e0010157 (2022). https://doi.org/10.1371/journal.pntd.0010157

Laing, E.D., Navaratnarajah, C.K., Cheliout Da Silva, S., Petzing, S.R., Xu, Y., Sterling, S.L., Marsh, G.A., et al.: Structural and functional analyses reveal promiscuous and species-specific use of ephrin receptors by Cedar virus. Proc. Natl. Acad. Sci. **116**(41), 20707–20715 (2019). https://doi.org/10.1073/pnas.1911773116

Lemkul, J.A.: From proteins to perturbed Hamiltonians: a suite of tutorials for the GROMACS-2018 molecular simulation package [article v1. 0]. Living J. Comput. Mol. Sci. (2018). https://doi.org/10.33011/livecoms.1.1.5068

Loomis, R.J., Stewart-Jones, G.B., Tsybovsky, Y., Caringal, R.T., Morabito, K.M., McLellan, J.S., Chamberlain, A.L., et al.: Structure-based design of Nipah virus vaccines: a generalizable approach to paramyxovirus immunogen development. Front. Immunol. **11**, 842 (2020). https://doi.org/10.3389/fimmu.2020.00842

Maar, D., Harmon, B., Chu, D., Schulz, B., Aguilar, H.C., Lee, B., Negrete, O.A.: Cysteines in the stalk of the Nipah virus G glycoprotein are located in a distinct subdomain critical for fusion activation. J. Virol. **86**(12), 6632–6642 (2012). https://doi.org/10.1128/jvi.00076-12

Marsh, G.A., Wang, L.F.: Hendra and Nipah viruses: why are they so deadly? Curr. Opin. Virol. **2**(3), 242–247 (2012). https://doi.org/10.1016/j.coviro.2012.03.006

Peel, A.J., Yinda, C.K., Annand, E.J., Dale, A.S., Eby, P., Eden, J.S., Jones, D.N., et al.: Novel Hendra virus variant circulating in black flying foxes and grey-headed flying foxes, Australia. Emerg. Infect. Dis. **28**(5), 1043 (2022). https://doi.org/10.3201/eid2805.212338

Plowright, R.K., Becker, D.J., Crowley, D.E., Washburne, A.D., Huang, T., Nameer, P.O., Gurley, E.S., Han, B.A.: Prioritizing surveillance of Nipah virus in India. PLoS Negl. Trop. Dis. **13**(6), e0007393 (2019). https://doi.org/10.1371/journal.pntd.0011126

Quarleri, J., Galvan, V., Delpino, M.V.: Henipaviruses: an expanding global public health concern? GeroScience **44**(5), 2447–2459 (2022). https://doi.org/10.1007/s11357-022-00670-9

Siegel, R.D.: Classification of human viruses. In: Principles and practice of pediatric infectious diseases, pp. 1044-1048.e1. Elsevier, Amsterdam (2018). https://doi.org/10.1016/B978-0-323-40181-4.00201-2

Sievers, F., Wilm, A., Dineen, D., Gibson, T.J., Karplus, K., Li, W., Lopez, R., et al.: Fast, scalable generation of high-quality protein multiple sequence alignments using Clustal Omega. Mol. Syst. Biol. **7**(1), 539 (2011). https://doi.org/10.1038/msb.2011.75

Skowron, K., Bauza-Kaszewska, J., Grudlewska-Buda, K., Wiktorczyk-Kapischke, N., Zacharski, M., Bernaciak, Z., Gospodarek-Komkowska, E.: Nipah virus–another threat from the world of zoonotic viruses. Front. Microbiol. **12**, 811157 (2022). https://doi.org/10.3389/fmicb.2021.811157

Sneha, P., Doss, C.G.: Molecular dynamics: new frontier in personalized medicine. Adv. Protein Chem. Struct. Biol. **102**, 181–224 (2016). https://doi.org/10.1016/bs.apcsb.2015.09.004

Stone, J.A., Nicola, A.V., Baum, L.G., Aguilar, H.C.: Multiple novel functions of henipavirus O-glycans: the first O-glycan functions identified in the paramyxovirus family. PLoS Pathog. **12**(2), e1005445 (2016). https://doi.org/10.1371/journal.ppat.1005445

Tamura, K., Stecher, G., Kumar, S.: MEGA11: molecular evolutionary genetics analysis version 11. Mol. Biol. Evol. **38**(7), 3022–3027 (2021). https://doi.org/10.1093/molbev/msab120

Taylor, J., Thompson, K., Annand, E.J., Massey, P.D., Bennett, J., Eden, J.S., Horsburgh, B.A., et al.: Novel variant Hendra virus genotype 2 infection in a horse in the greater Newcastle region, New South Wales, Australia. One Health **15**, 100423 (2022). https://doi.org/10.1016/j.onehlt.2022.100423

Turner, P.X.M.G.R.A.C.E.: Center for coastal and land-margin research. Oregon Graduate Institute of Science Technology, Portland (2005)

Wacharapluesadee, S., Ghai, S., Duengkae, P., Manee-Orn, P., Thanapongtharm, W., Saraya, A.W., Yingsakmongkon, S., et al.: Two decades of one health surveillance of Nipah virus in Thailand. One Health Outlook **3**, 1–14 (2021). https://doi.org/10.1186/s42522-021-00044-9

Wang, M., Cang, Z., Wei, G.W.: A topology-based network tree for the prediction of protein–protein binding affinity changes following mutation. Nat. Mach. Intell. **2**(2), 116–123 (2020). https://doi.org/10.1038/s42256-020-0149-6

Wang, J., Anderson, D.E., Halpin, K., Hong, X., Chen, H., Walker, S., Valdeter, S., et al.: A new Hendra virus genotype found in Australian flying foxes. Virol. J. **18**(1), 1–13 (2021). https://doi.org/10.1186/s12985-021-01652-7

Wang, Z., Dang, H.V., Amaya, M., Xu, Y., Yin, R., Yan, L., Hickey, A.C., et al.: Potent monoclonal antibody–mediated neutralization of a divergent Hendra virus variant. Proc. Natl. Acad. Sci. **119**(22), e2122769119 (2022). https://doi.org/10.1073/pnas.2122769119

Waterhouse, A.M., Procter, J.B., Martin, D.M., Clamp, M., Barton, G.J.: Jalview version 2—a multiple sequence alignment editor and analysis workbench. Bioinformatics **25**(9), 1189–1191 (2009). https://doi.org/10.1093/bioinformatics/btp033

Waterhouse, A., Bertoni, M., Bienert, S., Studer, G., Tauriello, G., Gumienny, R., Heer, F.T., et al.: SWISS-MODEL: homology modelling of protein structures and complexes. Nucleic Acids Res. **46**(W1), W296–W303 (2018). https://doi.org/10.1093/nar/gky427

Weingartl, H.M.: Hendra and Nipah viruses: pathogenesis, animal models and recent breakthroughs in vaccination. Vaccine: Dev. Ther. **5**, 59 (2015). https://doi.org/10.2147/VDT.S86482

Xu, K., Chan, Y.P., Rajashankar, K.R., Khetawat, D., Yan, L., Kolev, M.V., Broder, C.C., Nikolov, D.B.: New insights into the Hendra virus attachment and entry process from structures of the virus G glycoprotein and its complex with Ephrin-B2. PLoS ONE **7**(11), e48742 (2012a). https://doi.org/10.1093/protein/4.2.155

Xu, K., Broder, C.C., Nikolov, D.B.: Ephrin-B2 and ephrin-B3 as functional henipavirus receptors. In: Seminars in cell & developmental biology, vol. 23, pp. 116–123. Academic Press, Cambridge (2012b). https://doi.org/10.1016/j.semcdb.2011.12.005